Classical chaotic dynamics of two-dimensional electrons in a periodic antidot lattice

É. M. Baskin, A. G. Pogosov, and M. V. Éntin

Institute of Semiconductor Physics, Siberian Branch of the Russian Academy of Sciences, 630090 Novosibirsk, Russia

Two-dimensional electron billiards in the form of a simple square lattice of specularly scattering disks is investigated, where these disks are antidots in a magnetic field. The problem is developed into a study of "pinned" (not undergoing collisions) and collisional trajectories. The fraction of pinned trajectories is found analytically via computer simulation. The dynamics of the electrons on the collisional trajectories is investigated from the viewpoint of the theory of dynamical chaos. The fractal structure of the collisional trajectories in phase space is examined in the vicinity of the fixed points of the nonlinear map corresponding to stable regular motion, in particular to escape along a series of antidots, with this escape arising near isolated values of the magnetic field. The magnetic-field dependence of the components of the conductivity tensor is obtained with the help of computer simulation. It is shown analytically that geometrical resonances of the magnetoresistance are determined mainly by the escaping and near-lying trajectories leading to divergence of the kinetic coefficients in an ideal lattice. It is shown that in the limit of a weak magnetic field the main role in the transport is played by electrons moving at small angles with respect to the crystallographic directions. They give rise to the divergence of the conductivity in the absence of a magnetic field and the anomalous sensitivity of the kinetic coefficients to a magnetic field until the appearance of a negative Hall effect. © *1996 American Institute of Physics.* [S1063-7761(96)01012-8]

1. INTRODUCTION

Advances in technology have made it possible to create objects with characteristic dimensions approaching the wavelength of the electron. These include quantum dots, antidots, periodic lattices, microcontacts, rings, and wires. The study of these objects, which is undergoing vigorous development at the present time, has been stimulated by both applied and scientific problems. On the one hand, these objects can be considered as systems with artificial atoms, molecules, and nuclei, or as crystalline and non-crystalline solid bodies, thereby making it possible to model quantum phenomena taking place in natural systems. On the other hand, nanostructurization is necessary to reduce the dimensions of semiconductor devices and shorten their switching times.

Periodic antidot lattices were originally created in order to observe purely quantum effects, in particular the Hofstadter butterfly which describes the structure of the energy bands of a periodic lattice in a magnetic field, and the Aharonov–Bohm effect. Nevertheless, the dimensions of most of these structures exceed the electron wavelength, and therefore the first effect to show up in them is a purely classical phenomenon—geometric resonances of the magnetoresistance,[1-3] arising when the dimensions of the lattice are commensurate with the cyclotron diameter. The sharpness of these resonances is enhanced because the mean free path in these structures significantly exceeds the lattice period and the motion of the electron is ballistic.

The first explanation of geometric resonances, proposed in Ref. 2, was based on the appearance of pinned orbits which do not collide with the antidots. It only qualitatively agrees with the observed magnetoresistance: the large amplitude of the modulations of the magnetoresistance cannot be explained with such a model. The presence of pinned trajectories in a rigid potential with partial softening leads to the appearance of islands of stable, localized motion.[4] Fleischmann et al.[4] have pointed out the important role of stable delocalized ("escaping") trajectories and adjacent trajectories.

In the potential of a periodic lattice the variables describing the motion of the electron do not separate, as a rule. As a result, the motion of the electrons is quite complicated. Such problems are examined in the theory of dynamical chaos.

The present paper is dedicated to a systematic theoretical study and computer simulation of the chaotic classical dynamics of electrons in a periodic antidot lattice located in a magnetic field. The aim of this paper is to investigate the nature of the geometric resonances in the magnetic-field dependence of the kinetic coefficients by comparing the results of their computer simulation and analytical estimates.

We will use the model of a billiard table consisting of circular specular-scatterers located at the sites of a simple square lattice. It was on just such models that Sinaĭ et al.[5] based their well-known work.

In real heterostructures the free surface of a semiconductor creates for the electrons a repulsive bending of the bands near the surface. In thermal equilibrium the magnitude of this bending of the bands at the surface of the semiconductor is on the order of an electron volt, while the Fermi energy is on the order of 10^{-2} eV. In addition, the geometric dimension of the antidots is usually several thousand Ångstroms, which exceeds the thickness of the depletion layer, the Debye radius in a two-dimensional gas, which coincides with the Bohr radius, and the electron wavelength. Therefore, to a
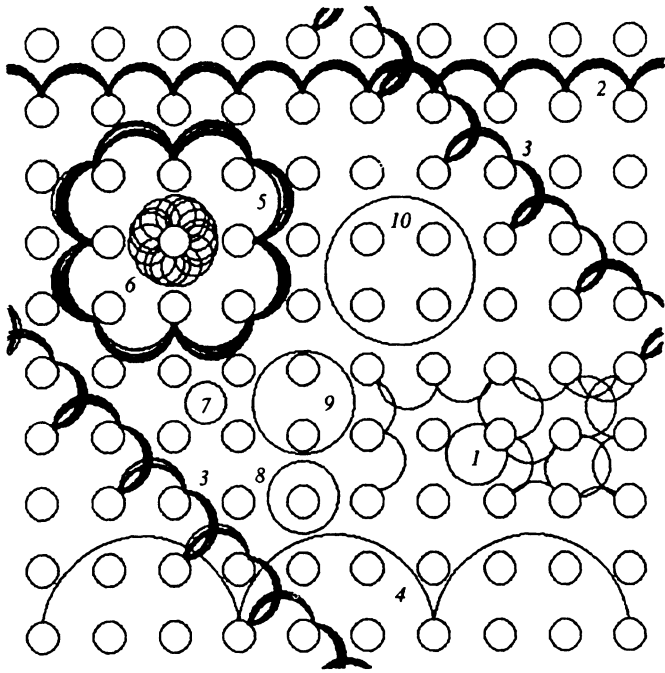
FIG. 1. Examples of different possible electron trajectories in a antidot square lattice in a magnetic field.

first approximation the potential in which the electron moves may be considered as the rigid boundary of the antidots.

In such a geometric formulation there is one characteristic dimensionless parameter—the ratio of the antidot radius a to the lattice constant d. We will examine the limit $a/d \ll 1$ in detail, bearing in mind that it is also applicable to the case $d - 2a \gtrsim a$. Only the case $d - 2a \ll a$, in which the system consists of narrow necks connecting massive open spaces, will remain beyond the scope of our treatment.

In billiard models all types of electron trajectories in the presence of a magnetic field can be divided into two independent groups. Figure 1 depicts some typical trajectories obtained by computer simulation. We may tentatively distinguish these trajectories as follows: $7-10$—pinned; 5 and 6—rosettes about one or several antidots; 1—ordinary diffusion; with trajectories $2-4$ corresponding to partially randomized but directed motion—the escaping trajectories.

Section II investigates pinned and escaping trajectories, which determine the properties of the kinetic coefficients. We will make use of statistical arguments to find the mean fraction of the pinned trajectories and its fluctuations for $a/d \ll 1$ in the limit of large cyclotron radius, $r_c \gg d$.

The collisional trajectories will be investigated by mapping the space of collision angles onto itself. This mapping leads to a fractal structure of phase space. Depending on the initial conditions, the electrons participate in either quasiregular or chaotic motion. Near the fixed points of the map of first and higher orders nonlinear resonances arise—regions of localized or escaping motion.

Motion near the fixed points corresponding to type-2 escape in Fig. 1, with which the geometric resonances of the kinetic coefficients are mainly connected, is investigated in detail. Computer simulation reveals the fine structure of the

dependence of the fraction of escaping and circumnavigating trajectories on the magnetic field for first-order resonances. Analytical estimates are made of the number of higher-order resonances and their phase area. The ratio of the number of higher-order resonances corresponding to escape and localization is found. The local and global symmetries of phase space are investigated.

Section III examines the components of the conductivity tensor in a magnetic field.

In moderate and strong magnetic fields we use the percolation approach for the analytical estimates of the mean conductivity. This approach replaces the periodic lattice by a disordered lattice. The presence of escaping trajectories leads to a divergence of the kinetic coefficients in an ideal lattice which is bounded when impurity scattering is taken into account. To find the contribution of the escaping trajectories to the conductivity, we use both the analytical and the simulation values of the fraction of these trajectories.

The case of a weak magnetic field is examined in close detail. The main role in the transport process in this limit is played by electrons moving at small angles to the crystallographic directions. They lead to a divergence of the conductivity in the absence of a magnetic field. As a result, the kinetic coefficients acquire an anomalously strong dependence on the magnetic field. Another consequence of this is a change in sign of the Hall effect. Results of the computer simulation are presented for the components of the conductivity and the magnetoresistance for different values of a/d and compared with results of the analytical approach.

2. ELECTRON DYNAMICS AND STRUCTURE OF PHASE SPACE

2.1. Pinned electron orbits

Pinned orbits can lie between antidots or enclose one, two, four, or more antidots. Shadowing decreases the size of the existence region of such trajectories and hinders the formation of trajectories enclosing a large number of antidots. For example, the existence region for pinned trajectories enclosing one antidot is defined by the inequalities $a < r_c < d - a$. In general, the existence conditions for pinned trajectories are prescribed by inequalities for the position of the center of the trajectory $\rho = x + iy$: if for all integers n and m the condition

$$r_c - a > |\rho - d_{n,m}| \quad \text{or} \quad |\rho - d_{n,m}| > r_c + a, \quad \text{or}$$

$$d_{n,m} = (n + im)d,$$

is satisfied, then any orbit with such ρ and r_c is pinned.

Figure 2 plots the fraction of unpinned (collisional) trajectories $f_s = 1 - f_p$ for different values of a/d as a function of r_c, obtained by computer simulation. Let us estimate the mean fraction of pinned trajectories f_p analytically. Toward this end, we neglect the regularity of the arrangement of the antidots. The probability of the appearance of pinned trajectories of length $2\pi r_c$ is equal to the probability that the electron will not collide with antidots having total scattering cross section $2a$: $\exp(-2\pi r_c/l)$, where $l = d^2/2a$ is the mean free path. As can be seen from Fig. 2, this estimate corresponds well to the average trend of the curve $f_c(r_c)$.
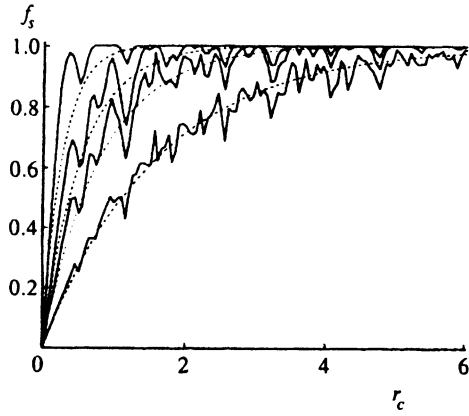
FIG. 2. Fraction of collisional electron trajectories f_s as a function of r_c in antidot square lattices with different a/d ratios: 0.05, 0.10, 0.15, 0.30 (smaller f_s correspond to smaller a/d). The dashed lines were calculated from the formula $f_s = 1 - \exp(-2\pi r_c/l)$.

FIG. 3. Fragment of an electron trajectory for two successive collisions with antidots.

However, for sufficiently large r_c the average behavior of this dependence deviates noticeably from what may be expected from this formula. The reason for this is that for large r_c the probability of the appearance of pinned trajectories in a regular lattice is significantly higher since for the center of the orbit symmetrically located in the cell it is sufficient for the particle to traverse without collisions not its entire circular orbit, but only a minimal sector of it, from which the entire orbit may be obtained by a symmetry transformation. As a result, the probability of the appearance of pinned trajectories with the center of the orbit, ρ, at various points in the cell is $\exp(-\pi r_c/Ml)$ where $M = 4$ at the points $(0,0)$ and $(1/2,1/2)$, $M = 2$ at the point $(0,1/2)$, $M = 1$ at the points $(0,y)$, $(1/2,y)$, $(x,\pm x)$, and $M = 1/2$ at all other points (x,y).

For $r_c \gg 1$ the greatest contribution to the total fraction of pinned trajectories comes from trajectories centered on the most symmetric points. To find the total fraction of pinned trajectories, we should interpret the meaning of the probability of the appearance of trajectories with prescribed position of the orbit center ρ. The weight of the symmetric points is related to the width of the maximum in ρ, which is determined by the condition that when the orbit center shifts by $\delta\rho$ new antidots fall inside the orbit or leave it. Hence $\delta\rho = d^2/4r_c$. This gives for the fraction of pinned trajectories

$$f_p(r_c) = \exp\left(-\frac{2\pi r_c}{l}\right) + 2\pi\left(\frac{d}{4r_c}\right)^2 \exp\left(-\frac{\pi r_c}{4l}\right). \qquad (1)$$

In addition to its smooth behavior, $f_s(r_c)$ undergoes irregular oscillations associated with geometric resonances. Singularities in f_s, are associated with the successive opening and closing of "windows" for the pinned trajectories. The first minimum of f_s corresponds to $2r_c = d$. Its depth is estimated as $8(a/d)^{3/2}/3$.

If $r_c \gg d$, then the number of "windows" for different pinned trajectories grows. For $2\pi r_c \lesssim l$ the windows overlap. For small a pinned trajectories arise between values of the cyclotron diameter that coincide with one of the values
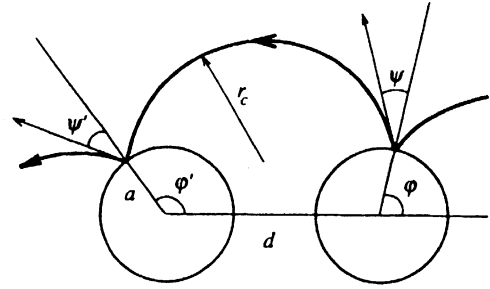
$$|d_{m,n}| = d\sqrt{m^2 + n^2}.$$

In light of the mutual irrationality of these numbers, the "windows" in r_c are distributed randomly and have random width (i.e., f_s is a fractal).

Each appearance of a new region of pinned trajectories is accompanied by a singularity of $f_s(r_c)$. Let such trajectories exist for some r_c. Then they necessarily disappear if for a small change in r_c inside the circle with cyclotron radius the number of antidots varies by one. This defines the width of a typical window for the existence of pinned trajectories of given type: $2\pi r_c \Delta r_c/d^2 \sim 1$.

For $r_c/l \gg 1$ the windows in r_c do not overlap. In this case they correspond, as a rule, to symmetric positions of the orbit center. Note that the interesting question of the statistics of the function $f_s(r_c)$ lies beyond the scope of the present work.

2.2. Collisional trajectories

An electron, having collided once with an antidot, will necessarily collide with it again if it does not first meet another. Therefore all collisional trajectories can be divided into localized rosettes and infinite trajectories.[1] As an electron moves along a rosette enclosing one antidot, the distance of the antidot to the center of the cyclotron orbit remains constant. For these trajectories to exist we must have $-a < \rho - r_c < a$. The condition of stability of rosette motion is $\rho + r_c + a < d$. Under this condition the electron will endlessly orbit around one antidot. From the kinetics standpoint these are localized states, which, like pinned states, in the absence of other scattering mechanisms do not take part in diffusion or longitudinal conduction. If the first of these two inequalities is satisfied and the second one is not, then the electron will complete rosette motion about one antidot as long as it does not run into another antidot, whereupon it will describe a rosette about it, etc. Delocalized trajectories appear for $2(r_c + a) > d$.

Motion of an electron is completely defined by two parameters: the angular position φ of the electron at the antidot (n,m) at the instant of the collision $(-\pi < \varphi < \pi)$ and its direction ψ after the collision $(-\pi/2 < \psi < \pi/2)$ (Fig. 3). The corresponding phase space is the direct product of a two-dimensional discrete space of coordinates of the antidot centers (n,m) and the two-dimensional ring of angular coordinates (φ,ψ). Motion of an electron in such a phase space is a mapping of this space onto itself $(\varphi,\psi,n,m) \rightarrow (\varphi',\psi',n',m')$:
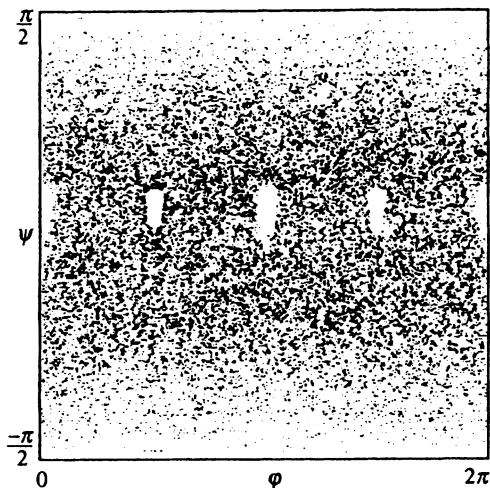
FIG. 4. Successive positions of an electron in the phase space of the angles φ, ψ, having started from an arbitrary point in the region of chaotic motion: $a/d=0.25$, $r_c=0.51$.
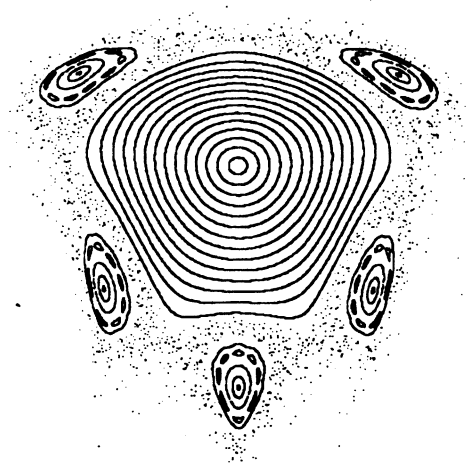

FIG. 5. Structure of phase space near a fixed point (corresponds to the unshaded regions in Fig. 4). Successive positions of an electron, having started from some initial point, form a closed contour. The various central contours correspond to different starting conditions. The satellite trajectories arise simultaneously. The randomly scattered points, corresponding to circumnavigating trajectories, were obtained for initial angles lying outside the closed contours.

$$ia[\exp(i\varphi')-\exp(i\varphi)]+r_c\{\exp[i(\varphi'-\psi')]$$

$$+\exp[i(\varphi+\psi)]\}=d_{n'-n,m'-m}. \qquad (2)$$

This equation has, as a rule, several solutions for φ', ψ', n', m' on one cyclotron orbit. We must choose the one that corresponds to the minimum angular distance from the initial point (φ,ψ,n,m) in the direction of motion along the cyclotron orbit.

The map (2) defines a complex structure in the phase space of these variables. For sufficiently small r_c, only motion along a rosette surrounding a single antidot is possible. In the $\varphi\psi$ plane such motion corresponds to jumps between successive points along the line ψ=const. For $d>2r_c>d-2a$ the lines ψ=const divide the region of angles corresponding to rosette motion from the remainder of the $\varphi\psi$ plane, where the motion is delocalized. For $2r_c>d-2a$, if the electron starts out from an arbitrary point in the $\varphi\psi$ plane, then subsequent points will cover the entire space with the exception of small regions near isolated angles. This is clearly visible in the total phase portrait, which depicts all successive coordinates (φ,ψ) of an electron that has started out from an arbitrary point (Fig. 4). The escaping trajectory 2 in Fig. 1 corresponds to unshaded region in Fig. 4 of $\varphi\psi$ space (enlarged in Fig. 5). A trajectory that starts out in this region remains inside it for an extended time.

For each collision with an antidot along such a trajectory the angles φ and ψ vary only weakly, i.e., they remain in the vicinity of a first-order fixed point of the map $\varphi'=\varphi=\varphi_0$, $\psi'=\psi=\psi_0$. If the electron starts out from the immediate vicinity of such a fixed point, the values of (φ,ψ) corresponding to successive collisions will describe an ellipse about this point. As the starting point moves further away from the fixed point, the nature of the motion changes: for the values of the parameters r_c, a, d we have chosen the initial ellipse transforms into five ellipses, each tightly surrounding a fifth-order fixed point. As the starting point

moves further away from the fixed point the motion becomes chaotic, so that after some number of collisions the depicted point escapes from the region under consideration. For these starting angles, memory of proximity to the fixed point is expressed in the result that over the course of these collisions motion in a prescribed direction is conserved. We call such trajectories circumnavigating trajectories and characterize them by the number of collisions preserving the direction of motion.

Between any two of the nested ellipses there exists an infinite number of high-order fixed points, each of which is enclosed in turn by smaller ellipses, as can be clearly seen for the ellipses enclosing the fifth-order points in Fig. 5.

Note that higher-order fixed points do not necessarily arise near a first-order fixed point as happens in the case of quadratic maps. For example, there exists a trajectory escaping along the diagonal in the [1,1] direction, corresponding to motion in the vicinity of a second-order fixed point.

The contributions of all of these trajectories taken together form the values of the kinetic coefficients. The pinned trajectories and the rosettes are localized and therefore do not contribute to the longitudinal conductivity, thereby decreasing the expected value. Relaxation is absent on the escaping trajectories, corresponding to an infinitely large decay time for the correlations. Consequently, they lead to a divergence of the kinetic coefficients. All remaining trajectories are diffusive and contribute in a regular way to the kinetic coefficients.

2.3. Symmetry of phase space

The general structure of phase space reflects the symmetry of the lattice. In a square lattice in a magnetic field the symmetry element is a rotation by $\pi/2$. This corresponds to the transformation $\varphi\to\varphi+\pi/2$, $\psi\to\psi$. In the total phase portrait this is reflected in a periodicity in φ with period

$\pi/2$. Near the stable points, as a consequence of the linearity of the map the symmetry is enhanced and a new symmetry element appears: $\varphi \rightarrow -\varphi$.

In addition to this secondary symmetry, the Poincaré sections possess a symmetry associated with invariance relative to the substitution $t \rightarrow -t$, $\mathbf{r} \rightarrow -\mathbf{r}$. As a result, we also have the symmetry $\varphi \rightarrow -\varphi$, $\psi \rightarrow \psi$ in the angles φ, ψ. This is clearly visible in the structure of the stability island in Fig. 5.

An additional symmetry, not associated with the symmetry of the lattice itself, arises in the vicinity of each fixed point of the map. As will be shown below, the satellite fixed-points in the vicinity of a first-order fixed point appear simultaneously. The appearance of satellites of fixed points determines the hidden symmetry of the stability islands.

The presence of hidden symmetry may be reflected in the physical properties of the system. This symmetry is different from crystalline symmetry. Therefore the symmetry of the kinetic coefficients could probe the symmetry of the stability islands if only it would be possible to isolate the contribution of an individual island. On the other hand, symmetry of higher order, e.g., fifth order, can influence only tensors of equally high rank and does not influence the static conductivity to which we will restrict ourselves in what follows.

The considered example of a fixed point is also distinguished by its symmetry with respect to $\pm \varphi$ since it corresponds to a symmetric point of phase space where $\varphi_0 = 0$. Escape is possible along any direction $[n,m]$. Only the directions $[1,0]$ and $[1,1]$ possess the symmetry $\mathbf{r} \rightarrow -\mathbf{r}$. The resulting fixed points and stability islands corresponding to this escape also possess this symmetry for these directions.

A picture analogous to escape also arises for the localized periodic orbits.

2.4. Analysis of the nonlinear map in the vicinity of a first-order fixed point

Escaping trajectories play the leading role in oscillations of kinetic coefficients. Therefore let us dwell on the nonlinear map (2) near one of the fixed points, e.g. (φ_0, ψ_0), corresponding to the above-mentioned trajectory 2 in Fig. 1.[2)]

The map (2) is a particular case of the nonlinear map of the two-dimensional plane $\mathbf{x}' = f(\mathbf{x})$. A smooth map can be investigated on the basis of the definition of the fixed points of the map and the expansion of $f(\mathbf{x})$ near them.

From the topological standpoint it is important that it be continuous. Note that formally this is not so. Breaks in the dependence of (φ', ψ') on (φ, ψ) appear as a consequence of the mutual shadowing of the antidots. However, it is not hard to see that a trajectory in real space depends smoothly on the initial conditions since shadowing begins when the trajectory touches an antidot. Let an electron successively collide with antidots 1, 2, and 3 and for some initial angles φ_1, ψ_1 touch antidot 2. Then according to Eq. (2) the angles (φ', ψ') undergo a jump, coinciding with φ_2, ψ_2 or with φ_3, ψ_3. At the same time φ_3, ψ_3 vary continuously. Therefore we may assume the map to be continuous.

The map linearized near a fixed point has the form

$$\mathbf{x}' = \hat{K}\mathbf{x}. \tag{3}$$

Because of conservation of phase volume the real matrix of the map, $\hat{K}$, is unimodular. Therefore the product of the eigenvalues λ_1 and λ_2 should be equal to unity, i.e., the cases of real eigenvalues of the form $\lambda_1 = 1/\lambda_2$ or complex eigenvalues of the form $\lambda_{1,2} = \exp(\pm i\gamma)$ are possible. In the first case the fixed point is unstable: after starting out in its vicinity the particle after a few steps arrives at a region where the linear map ceases to be valid. The second case is stable. In this case, successive values of $\mathbf{x}$ lie on an ellipse enclosing the fixed point.

The fixed points of the transformation (2) are $(\varphi_0, \psi_0) = [0, \pm\arccos(d/2r_c)]$. The first of these is stable, the second is unstable. Taking the parameter $(2r_c - d)/r_c$ to be small, we transform to the dimensionless variable $\mathbf{x}$:

$$(\varphi, \psi) = (\varphi_0, \psi_0) + \left(x_1 \sin\frac{\gamma}{2}, \ x_2 \cos\frac{\gamma}{2} \right)\frac{2a}{d},$$

where

$$\sin\frac{\gamma}{2} = \left[\frac{r_c(2r_c - d)}{a^2} \right]^{1/4}.$$

The matrix $\hat{K}$ has the form

$$\hat{K} = \begin{vmatrix} \cos\gamma & -\sin\gamma \\ \sin\gamma & \cos\gamma \end{vmatrix}.$$

Under the condition that $0 < r_c(2r_c - d) < a^2$, the matrix $\hat{K}$ reduces to a rotation of $\mathbf{x}$ through the angle γ about the fixed point. In the opposite case the angle γ turns out to be imaginary, and the map becomes unstable.

Due to incommensurability of γ and 2π, rotation in an arbitrary magnetic field leads to the result that after a long time the image points densely cover the circumference of a circle. For commensurable magnetic fields

$$\frac{r_c(2r_c - d)}{a^2} = \sin^4\left(\frac{m}{n}\pi \right)$$

and the trajectory consists of individual points located at the angles $\gamma = 2m\pi/n$.

For larger $\mathbf{x}$ small nonlinear terms must be added to the map (3):

$$\mathbf{x}' = \hat{K}\mathbf{x} + \hat{Q}\cdot\mathbf{x}\cdot\mathbf{x}, \tag{4}$$

($\hat{Q}$ is a dimensionless $2\times2\times2$ matrix), which have no effect on the motion as long as $\mathbf{x}$ is small.

For sufficiently large $\mathbf{x}$ the motion is distorted, which leads initially to a deformation of the ellipses and later to their breaking up into multiply connected curves and finally to chaotic motion. Since the map itself does not contain small parameters, the boundary of the stability region is estimated as $x \sim 1$.

In the particular case under consideration of escaping trajectories of type 2 in Fig. 1 and under the condition $a/d \ll 1$, the map (2) depends only on the parameter γ:

$$x_1' = x_1 \cos \gamma - x_2 \sin \gamma - \frac{1}{\sin(\gamma/2)}\left(x_1 \sin \frac{\gamma}{2}\right.$$
$$\left. + x_2 \cos \frac{\gamma}{2}\right)^2,$$

$$x_2' = x_1 \sin \gamma + x_2 \cos \gamma - \frac{1}{\cos(\gamma/2)}\left(x_1 \sin \frac{\gamma}{2}\right.$$
$$\left. + x_2 \cos \frac{\gamma}{2}\right)^2. \tag{5}$$

The stable fixed point $(0,0)$ and the unstable fixed point $[0, -2\sin^2(\gamma/2)/\cos(\gamma/2)]$ of the map correspond to cases already mentioned.

The effect of the nonlinear corrections in the map (5) grow as $|x|$ increases. At insignificant distances from the point $(0,0)$ most of the original circles, corresponding to a linear map, are only weakly distorted, remaining closed curves, i.e., the motion remains stable and periodic. At large distances from a fixed point new (not existing in the linear map) fixed points of higher orders arise (see Fig. 5). The reason for the appearance of satellite resonances can be understood if we take into account that according to Ref. 6 the influence of a nonlinear correction to the map reduces mainly to a dependence of the rotation angle γ on $|x|$. Thus, for certain values of $|x|$ the rotation angle becomes a multiple of 2π: $\gamma = 2\pi m/n$. This corresponds to satellite fixed points of nth order. In other words, after n rotations through the angle γ which is, generally speaking, incommensurate with 2π, the distance between the image and the original point is $|\delta x| \neq 0$. However, by increasing $|x|$, and consequently the effect of the nonlinearity shifting the image, it is possible to get it to coincide with the original point. This is well illustrated in Fig. 5, where the angle γ, which is close to $2\pi/5$, becomes exactly equal to $2\pi/5$ with increasing $|x|$, which leads to the formation of satellite fixed points of fifth order. With further increase of $|x|$ the stable motion is completely destroyed and becomes chaotic.

Such behavior is a particular case of the general scenario of destruction of invariant nonresonant tori, formulated in the Kolmogorov–Arnol'd–Moser (KAM) theorem. The existence of nonresonant closed trajectories of the map, incomprehensible from the standpoint of a discrete map, is easy to explain if we take into account the continuous dynamics of the particle. The space in question is a Poincaré section of phase space (intersection of a constant-energy surface with the antidot surface). A nonresonant torus in the two-dimensional case is two-dimensional, and its projection is a closed curve. According to the KAM theorem, a small perturbation does not destroy the nonresonant tori. The perturbation parameter is proximity to the fixed point. On the other hand, the resonant and destroyed nonresonant tori are located in the gap between the undestroyed nonresonant tori. This means that motion initiated between two nonresonant trajectories remains there perpetually. Destruction of a nonresonant trajectory leads to the appearance of both satellite ellipses and chaotic trajectories squeezed between nonresonant trajectories.

The order n of the main satellites is defined as $[2\pi/\gamma]$ (the integer part of $2\pi/\gamma$) or $[2\pi/\gamma]+1$ depending on which of the angles $\gamma[2\pi/\gamma]$ or $\gamma(1+[2\pi/\gamma])$ is closer to 2π. The magnitude of the rotation angle γ is determined by the control parameter H. Therefore the number of main satellites and, consequently, the symmetry of the stability regions varies discontinuously when the magnetic field is varied smoothly. If we choose the magnetic field such that the angle γ is close to $2\pi/n$ (nth-order linear resonance), then the influence of the nonlinear term grows. As a consequence, satellites arise at small values of x. The largest of these turns out to be an nth-order resonance.

Since each resonance generates satellites, the number of nth-order fixed points grows exponentially, and the size of the regions of stable motion tends toward zero. This means that the measure of the set of regions of n-periodic stable motion should depend on n nonexponentially, apparently as a power law.

In summary it may be said that a region of phase space exists corresponding to stable escape along series of antidots although inside this region the nature of the motion of the image point in phase space is quite complex. Inside this region there are connected and unconnected nonresonant trajectories, and also regions of chaotic motion, bounded by nonresonant tori. (By chaotic motion is meant the situation in which successive image points fill a set commensurate in the metric sense with the entire plane.)

The region of stable escape, generally speaking, is not connected. It is not hard to see that the outer boundary of this region, separating stable motion from chaotic, is irregular. It coincides with the last of the undestroyed nonresonant trajectories. Both the interior of the region of stable motion and its boundary are fractals: the first is a fractal since between each pair of undestroyed nonresonant trajectories destroyed ones are found, and the second—because its destruction proceeds through an infinite number of separatrices. Destruction of trajectories continues without limit, and this defines the self-similarity of the picture. If we color the region of escaping trajectories white, and the region of diffusive trajectories black, then in the terminology of fractal theory the white set is a Mandelbrot set and its boundary is a Julia set.[7]

The area of the Mandelbrot set is bounded from above by $2\pi^2$ (supremum) and from below by the area of the undestroyed nonresonant trajectory.

The circumnavigating trajectories occupy the immediate outer neighborhood of the Mandelbrot set. These trajectories are not formally distinguished from chaotic motion. However, a particle that has started out from this region will remain in the vicinity of the region of escaping trajectories for an extended period of time and conserve its directed motion. Moreover, motion along an escaping trajectory and motion along a circumnavigating trajectory near the Julia set are indistinguishable for an extended period of time.

Escaping trajectories are an analog of purely ballistic motion. Circumnavigating trajectories, being chaotic, can nevertheless lead to anomalously accelerated diffusion over the billiard table.

2.5. Fraction of escaping trajectories

The area of the region occupied by undestroyed nonresonant tori can be estimated if we require that the vector x located in this region not lie within the vicinity of a neighboring unstable fixed point. For $\gamma \sim 1$ this vector describes a nearly circular curve. This latter requirement means that $|x|$ should be less than 1. Consequently, the area of phase space corresponding to stable first-order escaping trajectories is

$$S_1(r_c) \sim (2a/d)^2 \pi u \sqrt{1-u^2} f(u). \qquad (6)$$

Here $f(u) \sim 1$ is a bounded dimensionless function of the parameter

$$u = \left(\frac{r_c(2r_c - d)}{a^2} \right)^{1/4}.$$

In terms of r_c the existence region of escaping trajectories is given by the inequalities $d < 2r_c < d + 2a^2/d$.

Strictly speaking, the indicated conditions determine the boundary of the stability region only approximately. Let us consider the boundary for the indicated interval. If we expand in γ and make the substitutions

$$\frac{\gamma}{2} x_1 \to x_1, \quad x_2 \to x_2 \quad \text{or} \quad \frac{\pi - \gamma}{2} x_2 \to x_2, \quad x_1 \to x_1$$

Eqs. (5) reduce to systems that do not contain γ

$$x_1' = x_1 - (x_1 + x_2)^2, \quad x_2' = 2x_1 + x_2 - (x_1 + x_2)^2$$

in the limit $\gamma \to 0$ and

$$x_1' = -x_1 - 2x_2 - (x_1 + x_2)^2, \quad x_2' = -x_2 - (x_1 + x_2)^2, \qquad (7)$$

in the limit $\gamma \to \pi$. From this it follows that if a region of stable motion exists, its dimensions and shape do not depend on γ and its dimensions are of order 1. If we continue r_c into the region $2r_c < d$, $d - 2r_c \ll d$, which corresponds to small complex γ, then the map (5) and the form of the curves do not change. As a result we can see that the boundary of the region of stable motion is somewhat wider than just mentioned.

Figure 6 plots the area S_1 of phase space occupied by circumnavigating trajectories as a function of r_c and the number of steps N along a series, over which the particle moves, obtained by computer simulation for $a/d = 0.25$. Since for small a/d the map (5) does not depend on a, these curves are universal. The limit $N \to \infty$ determines the area of the purely escaping trajectories as a function of the magnetic field. The maximum value of $S_1(r_c)$ and the width of its defining region agree with estimate (6).

In light of the appearance of linear resonances $\gamma = 2m\pi/n$, the curve $S_1(r_c, \infty)$ is a fractal. Its singularities are linked with the linear resonances (but do not strictly coincide with them). A clearly expressed minimum is visible in $S_1(r_c, \infty)$ at $r_c = 0.533$. It corresponds to $\gamma = 2\pi/3$. The other minima are near $r_c = 0.515$ and $r_c = 0.556$ ($\gamma = \pi/2$ and $\gamma = \pi$, respectively). The role of the linear resonances is also confirmed by the dependence of the shape of the stability islands on r_c: in the vicinity of these points their symmetry is of the corresponding order.
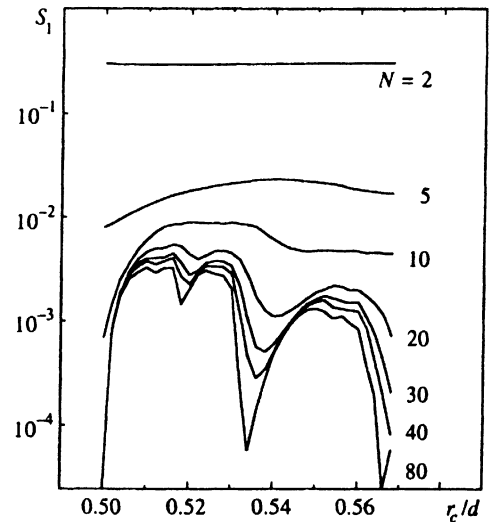

FIG. 6. Fraction of circumnavigating trajectories of the first period (type 2 in Fig. 1) as a function of r_c, calculated for different numbers of jumps N in the escape direction.

We gave special attention to the region near the threshold $2r_c = d$. Simulation shows that in this region as $N \to \infty$, $S_1(r_c, N) \to 0$ as $1/\ln N$.

We considered escaping trajectories jumping along the "peaks" of the antidots. Another type of escaping trajectory appears when the electron falls into a region of angles φ, ψ near the initial region of angles after several collisions with antidots. These trajectories correspond to fixed points of a higher-order map. They can be analyzed in the same way as those considered earlier if, omitting intermediate steps, we replace the nth-order map by a first-order map. It can also be linearized, we then add nonlinear terms, etc. As a result we get an infinite hierarchy of resonances.

Let us estimate the number of resonances of order n. Consider the multiple map at some point x_0. Then the image of some small increment Δx_0 will behave like $\Pi \hat{K}(x_n) \Delta x_0$. Of generally random matrices $\hat{K}(x_k)$, roughly speaking half correspond to real eigenvalues λ_k.

Let us consider the maximum value $|\Delta x_n|$. It is of the same order of magnitude as the product of maximum eigenvalues λ_n, i.e., it grows exponentially as $\exp(hn)$, where the Kolmogorov entropy is of the order of the volume-averaged instability growth rate: $h \sim \ln(l/a)$. In the particular case of a small magnetic field $h = \ln(d^2/2a^2)$ (Ref. 8). Since the map is continuous, the segment Δx_0 is imaged by some curve joining the ends of the segment Δx_n.

The characteristic dimension of x_n, as a function of x_0, δx_0, is defined by the last step of the map, which is the most sensitive to the initial conditions. Requiring that the increment Δx_n be of the order of the size of the cell, we obtain the characteristic dimension $\delta x_0 \sim \exp(-hn)$. Each cell of dimension δx_0 contains, as a rule, one stable fixed point of order n. Let x_0 be one of these points. Then for $\Delta x_0 < \delta x_0$ the map remains linear. Therefore the characteristic dimension of the region of stable motion is of the order of δx_0. Hence we may conclude that as for the higher-order satellite

resonances the product of the area occupied by the regions of stable motion by their number falls off more slowly than exponentially, apparently according to a power law.

Note also that the sensitivity of the resonance to variation of the magnetic field is mainly a result of the fact that the displacement of the trajectory in the first step of the map plays the role of a change in the initial condition for subsequent steps, i.e., $\delta r_c \sim \delta x_0$.

2.6. Higher-order localized and escaping trajectories

We have considered the case of escaping trajectories. A similar picture holds for localized periodic orbits. Let us estimate the ratio of the number of regions of localized and escaping motion of nth order. Toward this end, it is more convenient to consider the motion of the electron in terms of the coordinates of the centers of the cyclotron orbits. The phase plane of these centers is unbounded. The Hamiltonian of the system in these variables possesses the periodicity of the antidot lattice.

Scattering by an antidot leads to a change in the coordinates of the center of the cyclotron orbit of the order of r_c (if $2r_c > d - 2a$). This results in diffusion of the centers of the cyclotron orbits in two-dimensional space. A higher-order fixed point arises when as a result of diffusion the center of the cyclotron orbit falls onto the initial point or into an equivalent point (shifted by the lattice vector $d_{n,m}$) of the space of cyclotron orbit centers. The first case corresponds to localized motion, and the second to escaping motion. The ratio of the number of localized fixed points to the number of escaping fixed points of order n is equal to the probability that the orbit center will return to its original lattice cell after n steps.

Let us estimate the probability of return to the original cell, assuming that diffusion in these steps is not sensitive to the periodicity of the lattice. By doing so we are ignoring the anomalous character of diffusion in a regular lattice. Diffusion of the cyclotron orbit centers proceeds differently in moderate ($r_c \sim d$) and in very weak ($r_c \gg d$) magnetic fields. In a moderate magnetic field an orbit center revolves around one of the antidots during one collision time. After this a collision with another antidot takes place and the orbit center jumps a distance $\sim r_c$. In weak magnetic fields the electron jumps a distance $\sim l$ much less than r_c during a collision. The orbit center jumps a distance $\sim r_c$ in a circle around the spot where the electron is found. The accumulated small displacements of the electron lead to diffusion of the center of the cyclotron orbit along a circular band of width $l\sqrt{n}$. This picture is preserved as long as $l\sqrt{n} \ll r_c$ holds.

In the limit $l\sqrt{n} \gg r_c$ the magnetic field can generally be neglected in the description of the motion of the electron. The electron undergoes ordinary diffusion with its mean free path as the jump length. After n collisions the electron is displaced by the distance $l\sqrt{n}$. Since the orbit center is located a distance $r_c \ll l\sqrt{n}$ from the electron, the displacement of the orbit center after n steps is also $\sim l\sqrt{n}$ [accurate to within $r_c/(l\sqrt{n})$].

In order to wind up in the region of stable motion, the cyclotron orbit center must fall into some region ΔS. The

probability of doing this after n steps is equal to the ratio of ΔS to S_g, where S_g is the area swept out by the diffusion of the orbit center:

$$S_g = \begin{cases} 2\pi r_c l\sqrt{n} & \text{for} \quad l\sqrt{n} \ll r_c, \\ \pi l^2 n & \text{for} \quad l\sqrt{n} \gg r_c. \end{cases}$$

Stable motion, corresponding to localization, is achieved if the end-point lies in a lattice cell, the probability of which is equal to d^2/S_g. Escape takes place in the opposite case. Hence we obtain for the ratio of the fraction of localized to escaping trajectories after n steps

$$\frac{N_{loc}}{N_{run}} = \frac{d^2}{S_g - d^2} = \begin{cases} \dfrac{d^2}{2\pi l r_c \sqrt{n}} & \text{for} \quad l\sqrt{n} \ll r_c, \\ \dfrac{d^2}{\pi l^2 n} & \text{for} \quad l\sqrt{n} \gg r_c. \end{cases}$$

In the limiting case of moderate magnetic fields the electron, repeatedly colliding with an antidot over a time $\tau = d^2/(2 a v_F)$, describes a rosette around it. Here the center of the cyclotron orbit revolves around the antidot about a circle of radius $\sim r_c$, jumping a distance $\sim r_c$ after each collision with it. After colliding with another antidot, the electron begins to describe a rosette around it. Collision is equiprobable with any antidot inside the rosette. Thus, the orbit center jumps a distance $\sim r_c$. The diffusion coefficient is of the order of r_c^2/τ, which is typical for strong magnetic fields. The ratio of the fractions of localized and escaping trajectories is $d^2/(r_c^2 n)$.

Thus, in the limit $a/d \ll 1$, $r_c \gg d$ escaping trajectories are the main type of nonlinear resonance defining the properties of the kinetic coefficients.

3. CONDUCTIVITY IN A MAGNETIC FIELD

3.1. Strong field

To estimate analytically the components of the conductivity tensor in a magnetic field, let us forget for a moment about the periodicity of the antidot lattice. Then we may first invoke the formulas of kinetic theory and then make use of the percolation model[9] corresponding to a disordered system. Within the limits of applicability of the kinetic equation with a relaxation time, the components of the conductivity tensor in a degenerate Fermi system have the form

$$\sigma_{xx} = \frac{l_{tr}}{1 + (l_{tr}/r_c)^2}, \qquad \sigma_{xy} = \frac{l_{tr}^2}{r_c} \frac{1}{1 + (l_{tr}/r_c)^2}. \tag{8}$$

Here the conductivity is measured in units of $me^2 v_F/2\pi\hbar^2$, and the transport mean free path for specular scattering on the antidots is $l_{tr} = 3l/4$.

In Ref. 9 we showed that this model, typical for a three-dimensional system, is inapplicable to a two-dimensional system of randomly distributed point impurities. The point is that there are trajectories of the localized type (pinned and rosette) and, as a consequence, a threshold in r_c for the existence of delocalized trajectories. The system of randomly distributed antidots is analogous to an impurity system with antidot-scatterer concentration $N_a = d^{-2}$. The percolation

threshold r_c^0 in the problem of an aperiodic lattice of finite-size antidots is easily calculated as in Ref. 9:

$$\pi N_a[2(r_c^0+a)]^2=B_c,$$

where $B_c=4.4$ holds according to Ref. 10. As we saw earlier, in a periodic lattice a critical magnetic field also exists. The conductivity in a disordered antidot lattice can be found as in Ref. 9. If r_c is far from the percolation threshold, the conductivity can be estimated on the assumption that the contribution of the electrons colliding with the antidots and belonging to delocalized trajectories is determined by the kinetic equation. However, the non-colliding electrons do not contribute to the diagonal components, and their contribution to the nondiagonal conductivity corresponds to the ideal system. This means that when summing the contributions it is necessary to take account of the fraction of pinned trajectories $f_p(r_c)=\exp(-2\pi r_c/l)$. As a result we obtain

$$\sigma_{xx}=[1-f_p(r_c)]\frac{l_{tr}}{1+(l_{tr}/r_c)^2},$$

$$\sigma_{xy}=[1-f_p(r_c)]\frac{l_{tr}^2}{r_c}\frac{1}{1+(l_{tr}/r_c)^2}+r_cf_p(r_c). \qquad (9)$$

Formulas (9) are valid for $r_c \gtrsim r_c^0$ The numerically large value of the parameter 2π has the result that there exists a region of strong magnetic fields, $l\gg r_c\gg l/2\pi$, in which, on the one hand, the kinetic equation is applicable and, on the other, the role of the pinned trajectories is unimportant.

Let us proceed now to the case of a periodic lattice. Equations (9) give a valid description of the contribution of the chaotic trajectories and the mean number of pinned trajectories. To allow for fluctuations in f_p it is necessary to use Equations (9) and the results of Section 2.1. More important is the existence of escaping trajectories, which leads to an infinite conductivity for ideal periodic billiards. Inclusion of a finite impurity concentration destroys the periodic trajectories, bounding the conductivity by the mean free path l for scattering off the impurities. In this way the resonances are converted into maxima of σ_{xx} which are stronger, the lower the order of the resonance.

Lower-order resonances are possible only for isolated values of r_c comparable to d, which are manifested in geometric oscillations of the conductivity. Let us consider a first-order resonance. Moving along an escaping trajectory, the electron, before its next collision, traverses a path of length $2l_i/\pi$ (the factor $2/\pi$ appears due to the difference in the path-lengths along a semicircle and a straight line). This quantity plays the role of the mean free path of the escaping electrons. Let the contribution to σ_{xx} from a first-order resonance be denoted by $\sigma_{xx}^{(1)}$ This quantity is determined by the electrons belonging to escaping and circumnavigating trajectories.

The contribution of the escaping trajectories to the conductivity is $(2l_i/\pi)S_1(r_c)$. For the circumnavigating electrons the effective mean free path can be estimated as

$$l_{\text{eff}}=\left[\frac{1}{l_i}+\frac{2}{\pi Nd}\right]^{-1}.$$

Then their contribution to $\sigma_{xx}^{(1)}$ is given by

$$\int l_{\text{eff}}\frac{\partial S_1(r_c,N)}{\partial N}\frac{dN}{2\pi^2}\simeq\frac{2}{\pi}l_i\left[S_1\left(r_c,\frac{2l_i}{\pi d}\right)-S_1(r_c)\right], \qquad (10)$$

If the ratio $2l_i/\pi d$ is much greater than the characteristic dimension $S_1(r_c,N)$ as a function of N, then $S_1(r_c,N)$ converts to $S_1(r_c)$ and $\sigma_{xx}^{(1)}$ is determined by the escaping trajectories. In the opposite case the contribution of the circumnavigating electrons predominates and

$$\sigma_{xx}^{(1)}\simeq\frac{2l_i}{\pi}S_1\left(r_c,\frac{2l_i}{\pi d}\right).$$

Consequently, the curves in Fig. 6 describe the shape of the peak in σ_{xx} associated with a first-order resonance for various values of l_i.

The width of the peak in $\sigma_{xx}^{(1)}$ over r_c has the same order of magnitude $2a^2/d$ for any l. In the limits $2r_c\to d$ and $2r_c\to d+a^2/r_c$, the conductivity vanishes. In addition, $\sigma_{xx}^{(1)}$ has a fine structure that is associated with the linear resonances.

Simultaneous with this positive contribution to σ_{xx}, a negative contribution appears, associated with an increase in the fraction of pinned trajectories over the mean value in approximately the same fields. The amplitude of the fluctuation of the fraction of pinned trajectories $8(a/d)^{3/2}/3$ determines the amplitude of the relative fluctuation of the conductivity. It can be seen that the amplitude of the fluctuations of σ_{xx} due to a geometric resonance associated with escape is $l_i/l(d/a)^{3/2}$ times greater. The width of the fluctuational window in r_c for the pinned trajectories is significantly greater than for the escaping trajectories: $\Delta r_c\simeq d/\pi$. The superposition of these two effects can lead to additional fine structure of the main maximum of σ_{xx}.

Generally speaking, fluctuations in σ_{xx} can also be associated with higher-order escaping trajectories. For an nth-order resonance the directed motion is built up from individual series of n collisions each, where within each series the motion of the electron is purely diffusive. This means that escape takes place by way of individual jumps of mean length $l\sqrt{n}$, each completed during a time $\tau=nl/v_F$. The total number of collisions is equal to l_i/l. Consequently, the effective diffusion coefficient for an nth-order resonance is l_iv_F/n, and the average contribution from the kth order resonance is equal to $\langle\sigma_n^{(k)}(r_c)\rangle=l_iS_n(r_c)/n$, where $S_n(r_c)$ is the area in phase space of the vicinity of an individual nth-order resonance. As follows from an analysis of higher-order resonances, we have $S_n(r_c)\sim\exp(-2hn)$ and the width of the window in r_c for the existence of an nth-order resonance is $\Delta r_c\sim\exp(-hn)$. Consequently, the amplitude of the peak in σ_{xx} due to an individual nth-order resonance falls off exponentially faster than its width, and the contribution of an individual resonance spreads out with increasing order. Therefore, for large n the contribution to the conductivity of an individual resonance falls as $\exp(-hn)$.

The number of such resonances is equal to $\mathcal{J}(n)\sim S_n^{-1}$ The total area of phase space φ,ψ belonging to the stability islands is bounded from above by $2\pi^2$ (supremum). This means that the product $\mathcal{J}(n)S_n$ falls off as $n^{-\alpha}$ with $\alpha>1$ or faster. Assuming the usual power-law

falloff, we find that the total contribution to the product from an nth-order escaping trajectory falls off with n only as a power law:

$$\sigma_n = \sum \langle \sigma_n^{(k)}(r_c) \rangle \sim \frac{l_i}{n^\alpha}. \tag{11}$$

The width of the window in r_c does not vary; therefore the shape of the peak narrows. This effect becomes important in weak magnetic fields ($r_c \gg d$): In such fields, as a result of shadowing, resonances with small orders n simply do not exist.

Under such conditions, irregular fluctuations superimposed on the peak (11) may also show up, which are associated with the high order of the first of the destroyed resonances or, more accurately, with the exponentially large number of regions of phase space $\varphi \psi$ corresponding to this resonance. If we assume that their appearance is random and independent, then the root-mean-square fluctuation of their total contribution to the conductivity will be

$$\sqrt{\overline{(\Delta \sigma_n)^2}} \sim \frac{l_i}{n^\alpha} \exp(-hn). \tag{12}$$

Another reason for the appearance of fine structure in σ_{xx} at large r_c may be irregular fluctuations of f_s (see Fig. 2).

The motion of resonances whose order n is greater than l_i/l will be purely chaotic because of scattering from randomly distributed impurities. From the computer simulation standpoint a limiting factor is the length of a series of trials (number of collisions with antidots in each series). Therefore it is necessary to regard the simulation-generated dependences either as "fat" curves having a finite "thickness" associated with the fractality of the object, or as the result of some coarsening of the true dependences $\sigma(r_c)$. It may be anticipated turning on or turning off different types of escaping trajectories and localized trajectories as r_c varies determines the observed singularities in the dependence of the kinetic coefficients on the magnetic field.

Thus, taking impurity scattering into account imposes geometric resonances on the smooth curve $\sigma(r_c)$, and for $a/d \ll 1$ the escaping trajectories play a defining role. As the impurity scattering is decreased, finer and finer resonances gradually flare up.

3.2. Weak field

In this section we investigate the conductivity of an antidot lattice in the limit of a weak magnetic field. In a weak magnetic field the escaping trajectories are unstable. This is because for $H = 0$ the described billiard table is purely scattering and has no stable fixed points.[5]

An important property of a square lattice of antidots is the divergence of the diagonal conductivity. It arises because the electrons flying in singular directions hardly collide with any antidots. Essentially, this problem is equivalent to the problem of the conductivity of a thin film with a diffuse surface.[11,12] The latter, in the limit of a film thin in comparison with the bulk mean free path l, is proportional to $h \ln(l_i/h)$, where h is the thickness of the film. As $l_i \to \infty$, the

conductivity diverges. The role of the singular electrons for $H = 0$ is analogous to the role of the escaping electrons in a strong magnetic field; however, due to their instability the trajectories lead to a weaker logarithmic divergence.

To obtain the final value of the conductivity of an antidot lattice, it is important to take account of an additional scattering mechanism, e.g., that due to impurities. We will assume the impurity scattering length l_i to be significantly greater than the characteristic mean free path in the lattice $l = d^2/(2a)$. In addition, we will assume that the distance between the antidots $d - 2a$ is greater than or of the same order as the antidot radius a.

In an antidot lattice the role of a film is played by singular corridors. The characteristic width of a corridor is equal to $h = d - 2a$, and the characteristic angle of motion of an electron $\theta \sim h/l_i$. If this angle is much greater than a/d, then the electrons moving at a typical angle relative to the corridor "illuminate" an entire antidot and after colliding with it are scattered at large angles. Therefore the contribution to the conductivity of the electrons moving in the corridors is equal to $h \ln(l_i/h)$, i.e., the same as the conductivity of a thin film. This quantity must be multiplied by the probability that the electron is in the corridor, h/d. This argument is valid for $a/d \sim 1$.

If $h/l_i \ll a/d$, then only the peaks of the antidots are illuminated, which leads only to small-angle scattering off an antidot at angles of the order of $\sqrt{\theta d/a}$. It would seem that small-angle scattering leads to a slow relaxation of the momentum. However, this is not the case. The scattering angle significantly exceeds θ. Therefore, after a single scattering event the electron's mean free path is sharply reduced. The number of collisions the electron must undergo before it falls into the region of angles $\theta > a/d$ can be estimated if we continue the chain of equalities $\theta_{k+1} \sim \sqrt{\theta_k d^*/a}$, $d^* = d\sqrt{m^2 + n^2}$. Here m and n are the Miller indices for the corridor. Then, in the limit of large k we obtain an estimate for the number of collisions:

$$k \sim \frac{1}{\ln 2} \ln \frac{\ln(\theta_0 a/d^*)}{\ln(a/d^*)}.$$

In light of the very weak—doubly logarithmic—dependence of k on θ_0, we may take $k \sim 1$. The effective mean free path is built up from the mean free paths on all the steps. However, for small θ only the contribution of the initial mean free paths diverges when taking the angle average. In contrast to the problem of a film, for $a/d \ll 1$ only electrons with angles less than or of the order of a/d^* move in the corridor. Noting this restriction, we obtain for the contribution of the corridor to the conductivity

$$\sigma_{xx} \sim \frac{h^2 \sqrt{m^2 + n^2}}{d} \ln \frac{l_i a}{d^* h}. \tag{13}$$

It is necessary to sum the contributions from different corridors. For $a/d \sim 1$ the number of corridors is of the order of 1. For small a/d the number of corridors is large and is stipulated by the condition $d/\sqrt{m^2 + n^2} > 2a$. By definition of the Miller indices, the numbers m and n must be mutually prime. The sum must be taken over the half-plane $m > 0$. For large

m and n it can be replaced by an integral after multiplying the sum by the probability that the numbers m and n are mutually prime. This probability is given by the product of the probabilities that the numbers m and n are not simultaneously divisible $1 - 1/p_i^2$ by the prime numbers p_i,

$$P(m,n) = \prod_{p < \min(m,n)} \left(1 - \frac{1}{p_i^2}\right).$$

In the limit of large m and n the probability $P(m,n)$ can be expressed in terms of the Riemann ζ-function:

$$P(m,n) = \frac{1}{\zeta(2)} = \frac{1}{\pi^2 B_2} = \frac{6}{\pi^2}.$$

Replacing the sum over channels by an integral and allowing for the projection of the field onto the channel axis and for the current along the channel in the x direction, we obtain

$$\sigma_{xx} \sim \frac{\pi}{6} l \ln \frac{l_i}{l}. \tag{14}$$

Formula (14) shows that the order of magnitude of the conductivity is given mainly by the gas-kinetic formula $d^2/2a$, which is valid for randomly distributed antidots, but in contrast to it contains a logarithmic divergence. Note that the logarithmic divergence of the diffusion coefficient was pointed out earlier by Geisel et al.[13]

Formula (14) defines the mean conductivity of the system. Considered as a function of a/d, σ_{xx} undergoes jumps associated with the appearance of new corridors as a/d is decreased. The magnitude of the jumps is given by the expression (13).

The root-mean-square fluctuation of the conductivity is given by the product of the magnitude of a jump and the fluctuation of the number of corridors ΔN_{ch}. If we take the latter to be statistically random, then $\Delta N_{ch} \sim \sqrt{N_{ch}} \sim d/2a$.

Let us turn now to the case of a finite but small magnetic field. Since the conductivity is determined by small-angle electrons for $H = 0$, a quite weak magnetic field, drawing the electrons out of the corridor, substantially changes the conductivity. The characteristic field H can be estimated from the condition that the turning angle of the electron l_i/r_c during a collision time τ_i exceeds the characteristic angle of motion of the electrons, l/l_i. In the two limiting cases we obtain the following estimates for the conductivity:

$$\sigma_{xx}(H) = \sigma_{xx}(0) \left(1 - \frac{l_i^4}{r_c^2 l^2}\right) \quad \text{for} \quad \frac{l_i^2}{l} \ll r_c,$$

$$\sigma_{xx}(H) \sim \frac{1}{\pi} l \ln \frac{\sqrt{2ar_c}}{d} \quad \text{for} \quad l \ll r_c \ll \frac{l_i^2}{l}. \tag{15}$$

Let us turn our attention to the anomalously large value of the magnetic conductivity. For small fields it is determined by the parameter $l_i^2/r_c l$, which exceeds even the parameter l_i/r_c which determines the magnetoresistance of a sample without antidots.

For $r_c \sim l$ in the characteristic time an electron moves along a corridor the magnetic field manages to draw an electron out of the small-angle region, the small-angle contribution is no longer distinguishable, and formula (15) goes over

to the usual gas-kinetic expression. However, for $(\pi/4)r_c \lesssim l$ the possibility arises of pinned trajectories (Section 2.1.) since the probability of their appearance becomes non-exponentially small. As a result, geometric resonances appear in the dependence of σ_{xx} on r_c. A second (and more important) reason for their appearance is that the escaping trajectories, the simplest of them, as well as the pinned trajectories exist within the same windows in r_c.

Fleischmann et al.[14] showed numerically that in a weak magnetic field the Hall resistance changes sign. The special role of the channeling electrons can be seen in this behavior. The previous arguments allow us to obtain an estimate for the magnitude of the Hall conductivity in a weak magnetic field. We take $a/d \sim 1$. Let us consider the case $l_i \to \infty$. The electrons starting at angles $\theta \gg \theta_0 = \sqrt{2h/r_c}$ to the corridor axis (chosen, say, as the x axis) do not notice the magnetic field. In the opposite case, the magnetic field deflects the electrons starting from one series of antidots without allowing them to collide with another series. As a result of the first collision, the starting angle is significantly increased and the electrons go over to another group. Let the electric field point in the x direction. Then the number of electrons moving in the positive x direction exceeds the number moving in the opposite direction. After a collision the electrons are displaced in the y direction on the average by the distance h in the direction opposite the usual direction of drift in crossed fields. The magnitude of the contribution of the small-angle electrons to the Hall conductivity is

$$\delta \sigma_{xy} \sim -h \theta_0 / \pi \sim -h \sqrt{2h/r_c}. \tag{16}$$

For large r_c this contribution exceeds the conductivity associated with the remaining electrons h^2/r_c. Let us now turn our attention to the non-analytical dependence of $\delta \sigma_{xy}$ on the magnetic field.

3.3. Magnetoresistance

Let us consider the question of the magnetoresistance of the lattice. It is well known that in the degenerate case in an electron–impurity system magnetoresistance is absent since its appearance requires the presence of groups of electrons with different mobility, and the kinetic coefficients of a degenerate electron gas are determined by the electrons at the Fermi surface.

In a two-dimensional system the electrons separate into independent groups. As a consequence, even in a disordered system the magnetoresistance is nonzero. Substituting formulas (9) into the expression for the magnetoresistance

$$\rho_{ij} = \frac{\sigma_{ij}}{\sigma_{xx}^2 + \sigma_{xy}^2}$$

we obtain

$$\rho_{xx} = \frac{l_i(1 - f_p)}{f_p^2 r_c^2 + l_i^2}, \quad \rho_{xy} = \frac{1}{r_c} \frac{f_p r_c^2 + l_i^2}{f_p^2 r_c^2 + l_i^2}. \tag{17}$$

In a periodic lattice, to the groups of pinned and colliding electrons, we must add escaping and channeling. They also give rise to magnetoresistance.
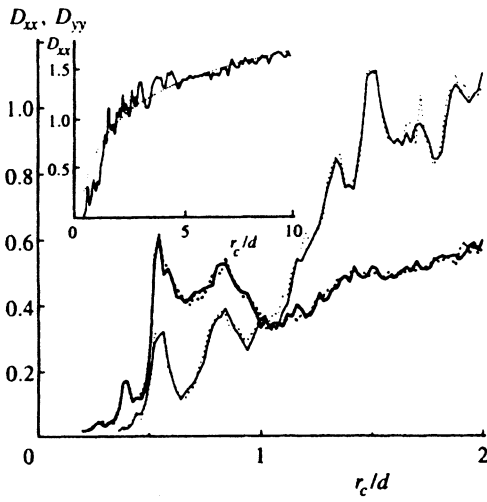
FIG. 7. Magnetic-field dependence of the components D_{xx} (solid lines) and D_{yy} (dotted lines) of the diffusion coefficient, obtained with the help of computer simulation in antidot lattices with $a/d=0.3$ (thick line) and $a/d=0.15$ (thin line). Inset shows the result of a calculation up to large r_c for a lattice with $a/d=0.15$; the dotted curve is a fit to these data based on relations (15) following the formula $D_{xx}=\ln(0.3r_c)+1.2$.

3.4. Computer modeling of kinetic coefficients

We performed a computer simulation of the kinetic coefficients for different values of the ratio a/d: 0.05, 0.1, 0.15, 0.25, 0.3, 0.4. We simulated the motion of a classical particle launched with random initial conditions in a lattice of specularly reflecting disks. The components of the conductivity tensor per particle with unit charge were calculated according to the formula

$$\sigma_{ij}=2\langle v_i(t=0)[r_j(t=\tau)-r_j(t=0)]\rangle. \tag{18}$$

Here $v_i(t)$ and $r_i(t)$ are the components of the velocity and position vectors, respectively, at the time t. The value of τ was chosen by means of a random number generator with a Poisson law and mean value of τ equal to 5 (in units of d/v_F), which simulated the finite scattering time of the randomly distributed impurities. 50 000 initial conditions, assigned with the help of the random number generator, were averaged over.

The simulation results are presented in Figs. 7–9. In a square lattice the diagonal components of the conductivity tensor σ_{xx} and σ_{yy} should coincide. The small difference between them, seen in Fig. 7, gives an estimate of the accuracy of the simulation. In all of the curves of σ_{xx} and σ_{yy} (Fig. 7) the peak at $2r_c\approx d$ is well expressed. Besides this, peaks at $r_c=0.8d$ are visible, and the minima in the conductivity between these two peaks are well expressed.

The main peak, obviously, is associated with the presence of trajectories near the escaping trajectories in the (0,1) and (1,0) directions. The second peak, presumably, is formed by the escaping trajectories of diagonal type.

The smoothing of the curves in the region of large r_c corresponds to the disappearance of escaping trajectories in such magnetic fields. In this case, for small values of a/d smoothing begins at large r_c (see Fig. 7), which is obviously connected with the lesser role of shadowing.
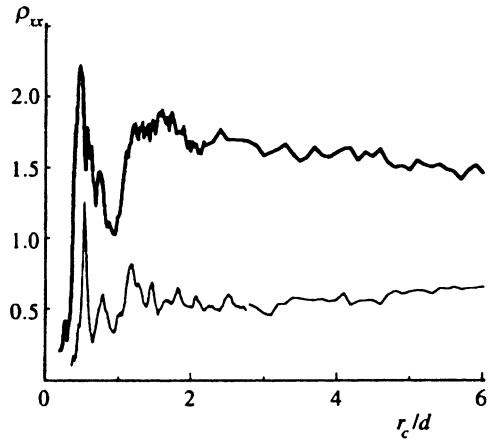

FIG. 8. Dependence of the longitudinal component of the resistance of an antidot lattice on r_c, calculated for two lattices with $a/d=0.30$ (thick line) and 0.15 (thin line).

As was noted above, the conductivity diverges logarithmically at large r_c [relation (15)]. According to relation (15) the smoothing of the dependence of σ_{xx} on r_c should be described by a logarithmic dependence. This is demonstrated by Fig. 7, where the points depict the dependence $\ln(0.3r_c)+1.2$ which has two fitting parameters.

In the region of intermediate magnetic fields $[r_c=(1-5)d]$ for $a/d=0.15$ irregular oscillations (Fig. 7, inset) are clearly visible, reflecting the fractality of the dependence of the kinetic coefficients on the magnetic field.

A similar picture of commensurate oscillations is also visible in the dependence of ρ_{xx} on r_c (Fig. 8). However, here the main peak at $2r_c=d$ turns out to be very sharply pronounced.

Results of calculation of the nondiagonal components of the conductivity tensor are shown in Fig. 9. The two main peaks of the curve $\sigma_{xy}(r_c)$ correspond to the peaks of the diagonal conductivity. However, they are shifted somewhat toward weaker magnetic fields. The reason for this shift within the context of the problem of periodically distributed
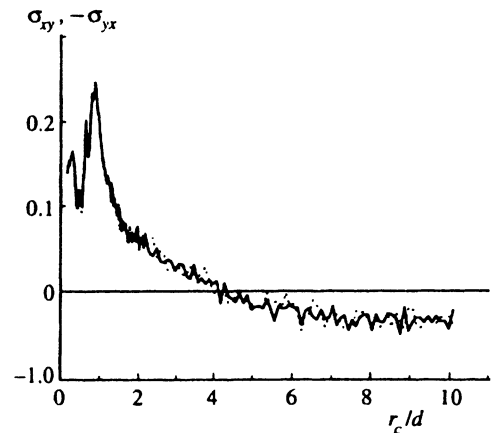

FIG. 9. Components of the Hall conductivity of an antidot lattice ($a/d=0.3$): solid line is σ_{xy}; dotted line is $-\sigma_{yx}$. For $r_c/d>4$ an anomalous negative Hall effect is observed.

scatterers is not clear to us. In addition, a strong maximum is observed at $r_c/d \approx 1$, corresponding to the minimum in the curve of $\sigma_{xx}(r_c)$ (Fig. 7).

An important feature of the nondiagonal conductivity is the change in sign at $r_c/d \sim 4$, which is clearly visible in Fig. 9. This supports the above arguments concerning the anomalous negative Hall effect.

It should be noted that our results for σ_{xy} differ strongly from the simulation results of Fleischmann et al.[14] In Fig. 9 we see clear maxima in place of the steps, as they obtained.

Conversion to the quantities ρ_{xx} and ρ_{xy} usually measured preserves the main features of the curves $\sigma_{xx}(r_c)$ and $\sigma_{xy}(r_c)$.

The above results coincide qualitatively with similar results obtained for lattices with other values of a/d. The comparison of the dependences $\rho_{xx}(r_c)$ for two different values of a/d, shown in Fig. 8, demonstrates that for smaller a/d a larger number of peaks is observed. This is due to the diminished role of shadowing effects.

The characteristic correlation scale of the dependence of the conductivity on r_c is equal in order of magnitude to the width of the region of stable trajectories $a^2/2r_c$.

4. DISCUSSION

Let us discuss the degree of generality of these results.

The entire analysis was carried out for a rigid antidot potential, where the antidot was modeled by a specularly scattering disk of finite radius. As was stated in the Introduction, the billiard model corresponds to antidot structures that now exist. At the same time, it is clear that it is also possible to create conditions for "soft" lattices. The question arises: which of our conclusions are model-dependent and which are general for any periodic lattice?

It is not hard to see that the breakdown of the trajectories into localized, chaotic, and escaping does not depend on the assumption of a rigid potential. Indeed, near the minima of a potential localized states always exist—less obvious is their appearance in a steep potential, where zero potential energy corresponds to undifferentiated equilibrium. However, in a magnetic field the appearance of localized trajectories is obvious.

Pinned trajectories, by definition, exist in a rigid potential. If we soften it, e.g., by considering a potential of the form $U_0[\cos(\pi x/d)\cos(\pi y/d)]^{2A}$, where A is sufficiently large,[4] then the pinned trajectories cease to be circular, but remain localized. The existence region of the localized trajectories turns out to be similar in shape and extent to the existence region of the pinned trajectories.

In order to demonstrate the possibility of escaping trajectories in a periodic lattice with a smooth potential, consider the intersection of trajectories of the opposite boundaries of a cell. Such an intersection obviously exists for some trajectories. It defines the mapping of the two-dimensional space of the initial position on the boundary and the angle of motion onto the space of final values of these parameters. It is clear that the idea of stable fixed points and stability regions of escaping motion is applicable to this map the same as to the map (2). Therefore the existence both of localized and escaping trajectories is a general property of motion in a

periodic potential. The conclusions about the higher-order fixed points also remain general, with the exception of the magnitude of the Kolmogorov entropy, which requires special calculation in such a problem.

The existence of escaping trajectories leads to anomalous diffusion in regular antidot lattices. Purely escaping trajectories, like ballistic trajectories, determine the displacement of the electron, which grows linearly with time. In this case, the formally introduced diffusion coefficient should also diverge linearly with time.

Since purely escaping trajectories are segregated in phase space from chaotic trajectories, it is of interest to elucidate the nature of the diffusion of the chaotic electrons. Our simulation, performed for $a/d=0.25$, $r_c/d=0.51$, shows that for these parameter values the diffusion coefficient also diverges with time, as $t^{0.2}$, i.e., weaker than for purely escaping trajectories. This divergence arises because the probability of capturing a trajectory into an almost localized state with an adiabatic trap or into an analogous circumnavigating state is high, where these adiabatic traps are regions of the initial conditions for which the electron remains within a bounded region of space for an extended period of time. It is mainly the latter state that is responsible for the divergence of the diffusion coefficient.

Wagenhuber et al.[15] performed a simulation of diffusion in the smooth periodic potential $U_0[2+\cos(2\pi x/d) +\cos(2\pi y/d)]$. They obtained step-like behavior of $D(t) \propto t^\beta$ with the exponent β varying from zero to unity as the parameter $(d/r_c)\sqrt{E_f/U_0}$ is decreased. According to this, it seems to us that such behavior is possible only in a transitional region for not too large t, whereas in the limit of large t the diffusion coefficient should behave linearly with time.

There are other questions that are in need of answers. How valid is the assumption of specular scattering by the antidots? In articular, how nonspecular are the boundaries of the depletion layer? How stable are the results if we allow for a small degree of disorder in the arrangement of the antidots and nonspecular scattering on them?

The boundary of the depletion layer is formed by a repulsive potential created by charged surface states. If the latter are associated with surface adsorption of atoms, the arising potential is random, i.e., the boundary of the depletion layer fluctuates. In addition, for technical reasons the geometrical boundary of the antidots is rough. The depletion layer smooths out these fluctuations, making them weaker than the relative fluctuations of the nascent antidot of charge and the roughness of the geometrical boundary. The results for escaping trajectories are stable to small deviations in the periodicity of the arrangement of the antidots and with respect to nonspecular scattering on them as long as the spread in the initial conditions due to these factors does not knock the electron out of the existence region of the escaping trajectories: $\Delta d/d$, $\Delta a/a < (a/d)^2$. Our estimates show that for $d \sim 1$ μm and $a/d=0.25$ these conditions are fulfilled.

ACKNOWLEDGMENTS

[1] In principle, rosettes exist surrounding several antidots as well as surrounding a single antidot; however, the former occupy an insignificant region of phase space.

[2] Analogous trajectories appear for $2r_c \simeq d_{m,n}$, $m,n > 1$. All that is said in the present section remains valid for them if we replace d $d_{m,n}$ and note that due to shadowing such trajectories do not always exist. Thus, for sufficiently large a the trajectories corresponding to $r_c \simeq d$ are forbidden. It is not hard to see that for small a and large m or n the simplest escaping trajectories arise in exactly the same magnetic fields as the pinned trajectories. However, the width of the windows for the escaping trajectories is smaller than for the pinned trajectories.

[1] K. Ensslin and P. M. Petroff, Phys. Rev. B **41**, 12307 (1990).

[2] D. Weiss, M. L. Roukes, A. Menschig, P. Grambow, K. von Klitzing, and G. Weimann, Phys. Rev. Lett. **66**, 2790 (1991).

[3] É. M. Baskin, A. G. Pogosov, and M. V. Éntin, JETP Lett. **55**, 678 (1992).

[4] R. Fleischmann, T. Geisel, and R. Ketzmerick, Phys. Rev. Lett. **68**, 1367 (1992).

[5] Ya. Sinaĭ, Usp. Mat. Nauk [in Russian] **25**, 141 (1970); Ya. Sinaĭ and Yu. Bunimovich, Commun. Math. Phys. **78**, 247 (1980).

[6] V. I. Arnol'd, *Mathematical Methods of Classical Mechanics*, 2nd ed. (Springer-Verlag, New York, 1989).

[7] H. O. Peitgen and P. H. Richter, *The Beauty of Fractals. Images of Complex Dynamical Systems* (Springer-Verlag, Berlin, 1986).

[8] G. M. Zaslavaskiĭ, *Chaos in Dynamical Systems*, Harwood Academic, New York (1985).

[9] É. M. Baskin, L. I. Magarill, and M. V. Éntin, Zh. Éksp. Teor. Fiz. **75**, 723 (1978) [Sov. Phys. JETP **48**, 365 (1978)].

[10] B. I. Shklovskiĭ and A. L. Efros, *Electronic Properties of Doped Semiconductors* (Springer-Verlag, New York, 1984).

[11] K. Fuchs, Proc. Camb. Phil. Soc. **34**, 100 (1938).

[12] J. M. Ziman, *Electrons and Phonons* (Clarendon Press, Oxford, 1960).

[13] T. Geisel, J. Nierwetberg, and A. Zacherl, Phys. Rev. Lett. **54**, 616 (1985).

[14] R. Fleischmann, T. Geisel, and R. Ketzmerick, Europhys. Lett. **25**(3), 219 (1994).

[15] J. Wagenhuber, T. Geisel, P. Niebauer, and G. Obermair, Phys. Rev. B **45**, 4372 (1992).

Translated by Paul F. Schippnick